remote sensing

MDPI

Article

Hierarchical Object-Based Mapping of Riverscape Units and in-Stream Mesohabitats Using LiDAR and VHR Imagery

Luca Demarchi [1,*], Simone Bizzi [1] and Hervé Piégay [2]

[1] European Commission, Joint Research Centre, Institute for Environment and Sustainability, Water Resources Unit, Via E. Fermi 2749, I-21027 Ispra, VA, Italy; simone.bizzi@jrc.ec.europa.eu

[2] UMR 5600 CNRS EVS, ISIG platform, University of Lyon, Site ENS de Lyon, 15 Parvis René Descartes, F-69362 Lyon, France; herve.piegay@ens-lyon.fr

* Correspondence: luca.demarchi@jrc.ec.europa.eu; Tel.: +39-0332-789-866

Academic Editors: Magaly Koch and Prasad S. Thenkabail
Received: 27 October 2015; Accepted: 18 January 2016; Published: 28 January 2016

Abstract: In this paper, we present a new, semi-automated methodology for mapping hydromorphological indicators of rivers at a regional scale using multisource remote sensing (RS) data. This novel approach is based on the integration of spectral and topographic information within a multilevel, geographic, object-based image analysis (GEOBIA). Different segmentation levels were generated based on the two sources of Remote Sensing (RS) data, namely very-high spatial resolution, near-infrared imagery (VHR) and high-resolution LiDAR topography. At each level, different input object features were tested with Machine Learning classifiers for mapping riverscape units and in-stream mesohabitats. The GEOBIA approach proved to be a powerful tool for analyzing the river system at different levels of detail and for coupling spectral and topographic datasets, allowing for the delineation of the natural fluvial corridor with its primary riverscape units (e.g., water channel, unvegetated sediment bars, riparian densely-vegetated units, *etc.*) and in-stream mesohabitats with a high level of accuracy, respectively of K = 0.91 and K = 0.83. This method is flexible and can be adapted to different sources of data, with the potential to be implemented at regional scales in the future. The analyzed dataset, composed of VHR imagery and LiDAR data, is nowadays increasingly available at larger scales, notably through European Member States. At the same time, this methodology provides a tool for monitoring and characterizing the hydromorphological status of river systems continuously along the entire channel network and coherently through time, opening novel and significant perspectives to river science and management, notably for planning and targeting actions.

Keywords: hydromorphology; object-based classification; LiDAR data; VHR imagery; machine learning; riverscape units; hierarchical classification

1. Introduction

The characterization of riverscape units requires monitoring water channels, in-channel morphological habitats, and riparian corridor structures and their interaction with the surrounding floodplain. Traditionally, these surveys require resource-demanding field campaigns supported, where available, by manual interpretation of aerial imagery [1,2]. Field surveys are often based on categorical information and expert-based opinions that may be biased by operators' subjectivity and inconsistency. These issues limit *de-facto* their operative implementation to a limited number of rivers (rarely extended to the entire river network scale), and may call into question their suitability for monitoring purposes, which demand an objective and repeatable assessment method. There is a pressing need for an operative, multi-scale framework for the evaluation of the hydromorphological

status of river systems [3]. This is especially the case for modern river management in Europe, where the Water Framework Directive (WFD) [4] acknowledges the major importance of fluvial geomorphology, requiring Member States to evaluate and monitor these types of forms.

Recent advances in Remote Sensing (RS) techniques are transforming the way we look at and analyze river systems and provide a new source of spatially distributed, multi-dimensional information at wider spatial and temporal scales compared to the past [5,6]. Thanks to RS datasets, hydromorphological indices nowadays can be estimated in a quantitative rather than descriptive way for multiple spatial scales—from reach and sub-reach units up to the entire basin—with continuous information that is more objective and less exposed to operator subjectivity [7–9].

An essential aspect when characterizing river hydromorphology is the delineation of the so-called active channel (AC) and more widely of different riverscape units [10]. The AC is defined in literature as the low-flow channel plus adjacent exposed sediment bar surfaces between established edges of perennial, terrestrial vegetation, which are generally subjected to erosion or deposition [10–13]. Exposed bars are characterized by vegetation encroachment, which plays a key role in the evolution of alluvial islands [14], *i.e.*, patches of mature vegetation surrounded by water and bare sediment bars. Sparsely-vegetated patches first appear in the island growth stage causing sediment accretion [15] and, if vegetation encroachment persists for long periods without being scoured during floods, it can transform a gravel bar into a forested or densely-vegetated island. Forested islands are distinguishable in fact by well-established and dense woody vegetation, which provides evidence of island stability [16].

A precisely delineated AC and mapped riverscape units (e.g., sparse vegetation units or densely-vegetated units) over time are important tools for understanding the morphodynamics of a river system. It also provides a useful indicator of changes in potential ecosystem productivity [10,17,18]. To date, the concept behind the use of RS for the delineation of the riverscape units has been rather simple: features visible on air photos can be manually traced or digitized and transferred to map coordinates [11,19,20]. Since the 1990s, the use of this technique has expanded rapidly, mainly because of the widespread availability of Geographical Information Systems (GIS), which made it much easier to digitize river features from aerial or satellite imagery. For example, Toone *et al.* [13] analyzed historical changes in channel morphology for the development of a geomorphological zonation of the Drôme river, over a period of 58 years based on a set of eight aerial photo-series. They digitized channel boundaries and extracted area and width parameters of the Total Active Channel (TAC), defined as the AC area plus any mid-channel islands or clusters of vegetation, on aerial photography.

Others have developed methods to semi-automatize the characterization of the low-flow channel using RS-based procedures, but not of other riverscape units [21]. Wiederkehr *et al.* [22] and Belletti *et al.* [10] measured AC width and island patterns of braided rivers in the French alps from aerial orthophotos from the 1950s to the 2000s with the aim of describing the present pattern and its evolution over 50 years. They both used eCognition Definiens® software, GEOBIA and decision trees on RGB orthophotos to map water, gravel bars and vegetation classes within the total active channel but did not focus on distinguishing the active channel from other floodplain units. At that time, the near-infrared band was not available for large coverages and the spatial resolution was not high enough to be suitable for this type of river application, making it difficult to distinguish vegetation patches from other channel corridor units. In the study by Bertrand *et al.* [8], water, vegetation, and gravel patches were mapped with an object-oriented classification approach, but based on band ratio and thresholding developed with expert-based rule-sets built on near-infrared and red bands of available orthophotos. Sediment bars within the channel were distinguished from arable crops, urban areas and mining sites found within the floodplain, according to their distance to the floodplain centerline and neighboring objects (e.g., low-flow channel and riparian vegetation previously detected). In this way, it was possible to delineate the active channel as the ensemble of water channels and unvegetated sediment bars, and to provide spatially-distributed information for some riverscape units continuously over the entire Drôme River Basin (France, 1680 km^2). This method is case specific since it is driven by

expert-based rule-sets and thresholds and it does not automatically distinguish the active channel and its main riverscape units.

Within the water channel, identification of in-stream mesohabitats is also important. These spatial units represent specific combinations of hydrodynamic and morphological conditions, which can be linked to distinctive habitats and ecological niches [23]. In the habitat classification of Frissell *et al.* [24], they are related to the concept of functional river habitat. At the same time, the European Habitats Directive (92/43/EEC) [25] aims to mitigate hydromorphological alterations that affect river ecosystems by implementing habitat enhancement and river restoration actions to benefit aquatic species [26]. Mapping mesohabitat distribution over a river's entire length is of key relevance for quantifying the ecological responses of aquatic organisms to hydromorphological alterations [23,27].

Regarding mapping in-stream mesohabitats with RS data, Wright *et al.* [28] classified stream habitats using imagery with 4 spectral bands acquired at 1 m ground resolution with supervised classification procedures, however, it resulted in low accuracies (between 10% and 53%). Legleiter *et al.* [29] tested the effects of sensor resolution on mapping mesohabitats. They achieved the best overall accuracies of about 60% for four habitat types, showing that reasonable accuracies were obtained only when using hyperspectral data and that accuracy was significantly higher with 1 m pixels compared with 2.5 m pixels. The spectral resolution was shown to be more important than spatial or radiometric resolution for this specific purpose [29]. Marcus *et al.* [30] mapped the main in-stream habitats using hyperspectral data with an accuracy ranging from 68% to 86%. For the first time, they showed that in-stream features mapping using RS data of very high spectral resolution can be more accurate than field crew surveys. More recently, Wiederkehr *et al.* [22] using the GEOBIA approach and discriminant analysis, were able to map in-channel mesohabitats (e.g., riffle, pool, lentic/lotic channel, gravel bench and shaded areas) for the lower Drôme river, with an overall higher accuracy: 90% of polygons were correctly classified, with less accurate identification of riffles (64%).

Currently, there is no a tool that automatically maps and characterizes riverscape, riparian, and mesohabitat units from RS data in proper geomorphological terms. The major research challenge consists of automatically distinguishing the riverscape units that are within the active channels (AC) from other landscape features found within the floodplain. Sediment bars, arable bare soil fields or human-made surfaces all present similar spectral reflectances. Likewise, sparsely-vegetated patches within the active channel and crop fields found in the external part of the floodplain are easily confounded. At the same time, different kinds of in-stream mesohabitats present subtle spectral differences. Hyperspectral data have notable potential to overcome both issues [30–32], however its availability is limited, especially for large-scale applications, whereas, combining spectral data with other sources of RS data, such as topographic data, might help in achieving this goal.

In this paper, we investigate the potential of very high resolution (VHR) near infrared aerial imagery (0.4 m) and LiDAR-derived products for mapping riverscape units and in-stream mesohabitats. For this purpose, we employed a database composed of VHR and LiDAR-derived products that were simultaneously acquired in 2009–2010 and available at the regional scale for the Piedmont Region in Italy (25.387 km^2). We present a new, semi-automated methodology, based on the integration of the spectral and topographic information within a multilevel geographic, object-based image analysis (GEOBIA). The ability of GEOBIA to couple the high spatial resolution of VHR imagery and the high-resolution topography of LiDAR were tested along a 45-km section of a gravel-bed alpine river (Orco River, tributary of the Po River). High resolution multi-spectral datasets and LIDAR derived topography are starting to be accessible to most countries in Europe, covering large areas and opening the possibility to attempt basin, and beyond regional scales hydromorphological characterization [33]. Being able to semi-automatize this task deriving continuous, objective and repeatable measures would support the monitoring of active channel changes and associated dynamics of riverscape units, fostering managers and scientists to interpret river processes with an unprecedented level of accuracy and therefore providing novel opportunities to understand fluvial processes and to support their management.

2. Study Area and Data

2.1. The Orco River

The Orco River is a large Italian stream originating on Gran Paradiso Mountain at 3865 m above sea level, located between the Aosta Valley and Piedmont regions in northwest Italy. After flowing for approximately 80 km, it enters the Po River. The Orco River drainage basin area is about 900 km^2, and contains the most important hydroelectric complex in the Piedmont Region, consisting of five hydropower dams. It is characterized by a relatively high perennial discharge, ranging from 13 m^3/s in February to 45 m^3/s in June [34]. The Orco River is an alpine, gravel-bed, high-energy river with a single-thread, sinuous channel (meandering) in the upstream part of the catchment. Downstream, just forty km before joining the Po River, the channel begins to wander and becomes multi-threaded with vegetated and unvegetated sediment bars, where the valley floor is wider (see Figure 1).

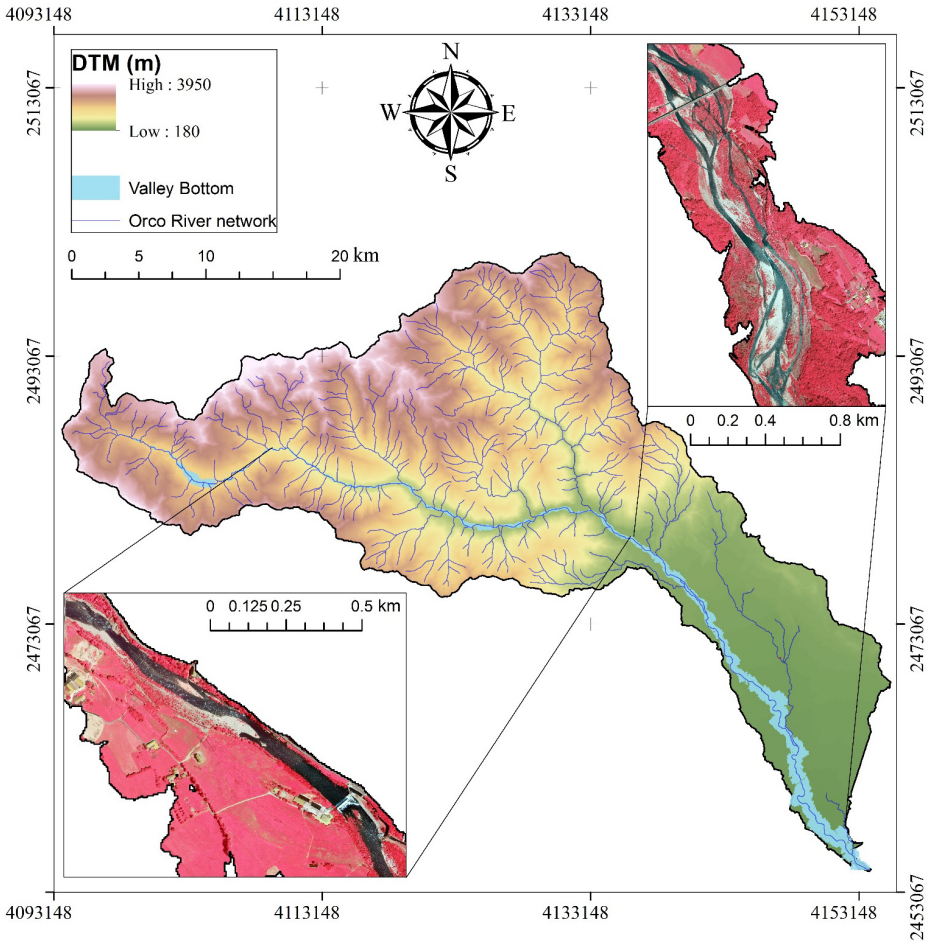

Figure 1. Orco River study area. The valley bottom layer (**light blue**) locates the 45-km river stretch analyzed. In the first upstream part the channel is single thread and sinuous (see representative orthophoto on the **bottom left**). In the downstream part, the river becomes wandering (see representative orthophoto on the **top right**).

During the 20th century, the river experienced severe riverbed incision, particularly in its downstream reaches due to gravel mining activities, dam construction and landuse changes that occurred in the basin [35]. As a consequence of riverbed incision and bank stabilization, the wandering multi-threaded river stretch was transformed into a single-thread, sinuous configuration. This progressive simplification of the fluvial pattern resulted in the abandonment of secondary channels, the joining of islands into the surrounding floodplain, and a significant deepening of the riverbed

(1–2 m on average and a local maximum of 3.5 m). Gravel mining activities have been regulated and limited over the past decades and this phase of riverbed incision has recently progressively decreased. Severe floods occurred in 1993 and 2000, which significantly modified the channel geometry, leading the river to recover its wandering pattern. Indeed, in some river reaches, old channels were reactivated and the active channel widened [36]. In this study, we focused on a 45-km section of the Orco River, representing both river types: the single-thread sinuous channel in the upstream part and the mostly wandering reach in the downstream part (see Figure 1).

2.2. Classification Process: Riverscape Units and in-Stream Mesohabitats

The main units describing the riverscape environment that were mapped in this study are listed in Table 1 and shown in Figures 2 and 3. Level 1 units were classified in Step 1 of the riverscape units classification workflow, based on automated Machine Learning classification (see Section 3.1). A higher level of detail (Level 2) was defined for the in-stream mesohabitats and for other vegetated units of the riverscape. Part of this classification step was carried out in Step 2 of the riverscape units classification workflow based on expert-based post-classification rule-sets (see Section 3.1).

Table 1. Classification scheme adopted in this paper to map the main units describing the riverscape environment.

Land-Cover Class		Class Description
Level 1	***Level 2***	
Water Channel (WC)—part of the AC	Pools	Areas with a gentle surface slope and slow flow.
	Riffles	Areas of swifter-flowing water.
	Runs	Areas of fast-moving, non-turbulent flow.
	Standing Waters	Surface water relatively still.
Unvegetated Sediment bars (US)—part of the AC		Sediment bars without vegetation.
Sparsely-Vegetated units (SV)—part of the Total Active Channel	Sparsely-Vegetated units of Islands (SVI)	Sparse vegetation units entirely surrounded by WC and/or US.
	Riparian Sparsely-Vegetated units (RSV)	Riparian sparse vegetation units adjacent to (but not surrounded by) WC and/or US.
FloodPlain units (FP)	Densely-Vegetated units of Islands (DVI)	Dense vegetation units entirely surrounded by WC and/or US and/or SVI.
	Riparian Densely-Vegetated units (RDV)	Riparian dense vegetation units adjacent to (but not surrounded by) WC and/or US and/or RSV.
	Other Floodplain Units (OFU)	All remaining floodplain units

An exhaustive description of riverscape units includes all landscape elements directly affected by fluvial processes, these include the FloodPlain units (FP) and the morphological active channel, named Active Channel (AC). FP compose the valley bottom and are most often composed of alluvial sediments. FP link the AC with surrounding terraces or hillslopes. The AC, as briefly discussed in the Introduction, is composed of the low-flow Water Channel (WC) and Unvegetated Sediment bars (US), which frame the active part of a river channel that is continuously reworked by dominant floods (e.g., 1-in-2 year floods). Here, we also define the Total Active Channel (TAC) as the AC plus units of Sparsely-Vegetated sediment (SV), *i.e.*, sediment bars which show indications of vegetation encroachment. The process of encroachment plays a key role in the evolution of alluvial islands [14], *i.e.*, patches of mature vegetation surrounded by water channel and bars of bare sediments.

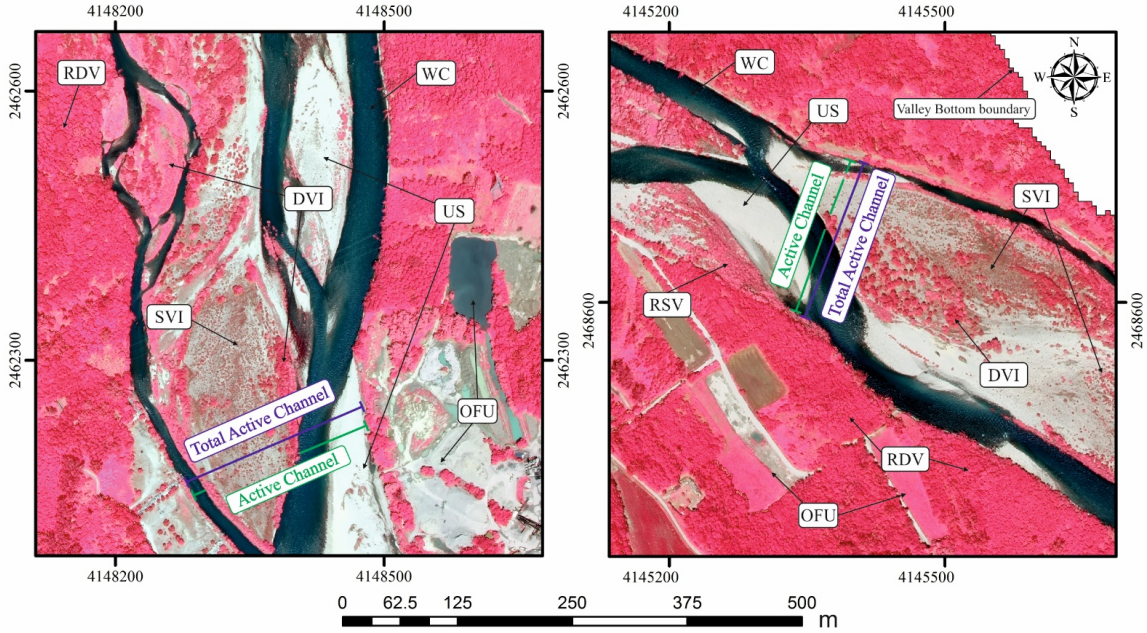

Figure 2. Examples of visible riverscape units on the Orco River (Italy) from VHR imagery (false color composite). For class codes, refer to Table 1.

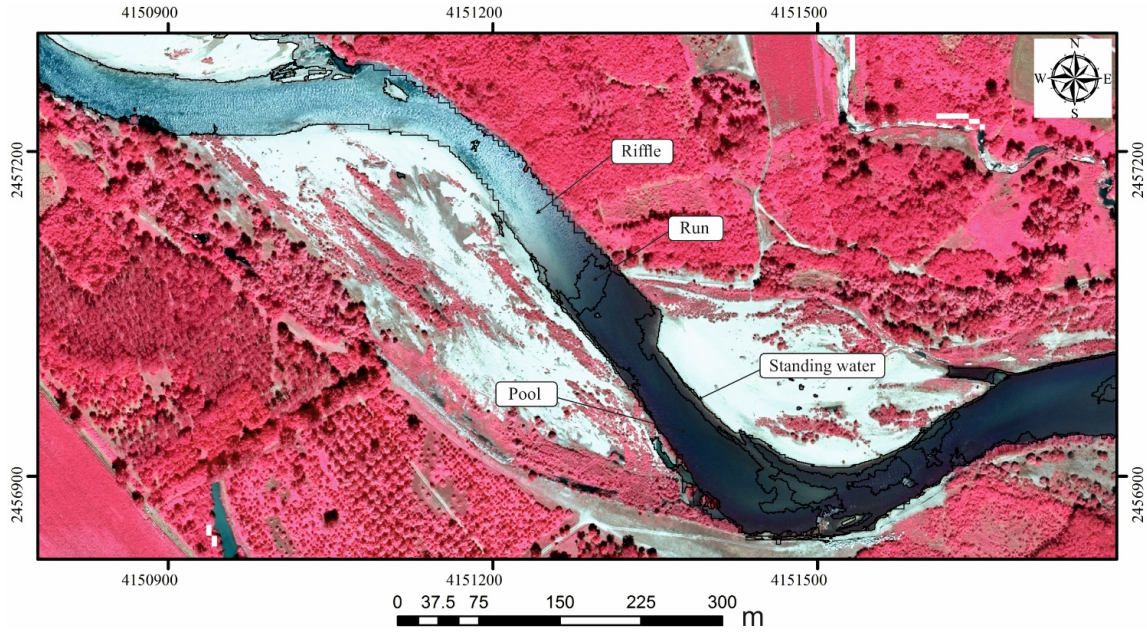

Figure 3. Examples of visible in-stream mesohabitats on the Orco River (Italy) from VHR imagery (false color composite).

Precise delineations of the AC, TAC and FP are of great importance. Such classification allows distinguishing the area of the channel regularly reworked by floods from, if present, FP that are hydrologically connected with the river but where vegetation and morphology are not primarily controlled by fluvial processes. AC, TAC and FP can be further subdivided into a number of sub-units, each associable to specific hydromorphological processes and forms. The Sparsely-Vegetated units (SV) can be subdivided into riparian (RSV) and island (SVI), if surrounded by WC and/or US, while within the FP it is possible to identify Riparian Densely-Vegetated units (RDV) and Densely-Vegetated units of Islands (DVI) from Other Floodplain Units (OFU) (Figure 2). SVI and DVI are usually found

within the active channel boundaries and therefore are entirely surrounded by WC and/or US. On the other hand, RSV and RDV are vegetation units adjacent to the active channel, but not entirely surrounded by it (Figure 2).

The major challenge of mapping riverscape units composing AC and TAC automatically from remotely sensed data lies in distinguishing them from other landscape features found within the floodplain (FloodPlain units class). Densely-Vegetated units of Islands (DVI) need to be differentiated from the densely-vegetated areas found within the floodplain and belonging to the OFU class. At the same time, Sparsely-Vegetated units of Islands (SVI) present very similar characteristics to crop fields found within the floodplain and characterized by an intermediate level of vegetation growth, clearly visible from Figure 2. Furthermore, Unvegetated Sediment bars (US) are spectrally comparable to crop fields left fallow due to crop rotation practices, but also to the mining activities that can be found in the floodplain (FP class, Figure 2). Similarly, gravel rural roads or urban settlements are found within the floodplain and belong to the FP class. Parsing the spectral similarity between urban areas and bare soil fields is a huge challenge, even for RS data operating at high spatial and spectral resolution (e.g., hyperspectral data) [32,37–39]. In this study, the use of topographic information coupled with spectral data was designed to provide a valuable support for the automatic classifier, since morphological features in the floodplain are normally characterized by higher elevation compared to those in the active channel where erosional processes take place during floods.

The Water Channel can be further classified into in-stream mesohabitats (Level 2, Table 1), *i.e.*, patches of surface water characterized by specific hydrodynamic features. Similarly to Marcus *et al.* [30], we identified four visible mesohabitat types: Riffles, Pools, Runs and Standing Water (see Figure 3). Riffles are areas of swifter flowing water, where the surface is turbulent. They represent topographic high points in the bed profile and are composed of coarser sediments. At base flows, they are shallow and have a steep water-surface gradient with rapid flow. In contrast, Pools are deeper and generally have a gentle surface slope with slower flow. They represent low topographic points with finer substrates. A Run is a relatively shallow portion of a stream characterized by relatively fast-moving, non-turbulent flow. Standing Water is a patch of the surface water that is relatively still at the interface between flowing water and a sediment bar. Identification of these classes has long been a problem, because different kinds of in-stream habitats present subtle spectral differences.

2.3. Remote Sensing and GIS Input Data Preparation

During the years 2009/2010, the Regione Piemonte commissioned an acquisition campaign to cover the entire region (25,400 km^2) with 40 cm near-infrared orthophotos coupled with simultaneous topographic LiDAR data acquired at an average point density of 0.4 point/m^2. The 45-km section of the main Orco River analyzed in this study corresponds to a mosaic of eleven tiles of 6.7-by-5.7 km each, which was projected into the Lambert azimuthal equal-area projection (LAEA) in order to fulfill the INSPIRE Directive requirements [40]. The different sources of RS and GIS data used for this study are summarized in Figure 4; dotted lines indicate processes carried out by the authors, while solid lines indicate external processes made available to the authors for the input data preparation.

The Red and Near-infrared spectral bands (2 and 3, Figure 4) were used by the authors to calculate the Normalized Difference Vegetation Index (NDVI) (4, Figure 4). The data provider executed the post-processing of the LiDAR points cloud acquired during the flight, generating a Digital Terrain Model (DTM) of 5 × 5 m grid cells (5, Figure 4). A quality check was also performed by the data provider, which resulted with an error of ±0.3 m in both vertical and horizontal directions. The authors used the DTM to calculate the Slope (6, Figure 4) using the Zevenbergen–Thorne method [41]. The "*Fluvial corridor*" toolbox described in Roux *et al.* [42] was adopted by this study for the delineation of the Valley Bottom (8, Figure 4), defined as the modern alluvial floodplain by Alber and Piégay [9]. It is a crucial fluvial unit in the bio-geomorphic characterization of stream networks [43] because it represents the deposition zone of alluvium, including both riverbed and floodplain areas. All analyses performed within this study are focused within the boundaries delineated by the Valley Bottom

shapefile and therefore all raster-based data described in Figure 4 were accordingly clipped, ignoring everything that fell outside of these boundaries. The "*Fluvial corridor*" toolbox was also employed for the calculation of the Detrended Digital Terrain Model (DDTM), by using the Orco River centerline shapefile and the DTM. As a first step, the stream elevation was extracted along the fluvial network with a constant spatial step (disaggregated network). The DDTM was then obtained by subtracting the stream elevation from the original DTM (7, Figure 4) for each pixel within the floodplain. The DDTM is necessary to represent the elevation of all floodplain pixels compared to the river network, and if it is well-fitted, it can be essential in distinguishing different geomorphic features (see Section 4.1).

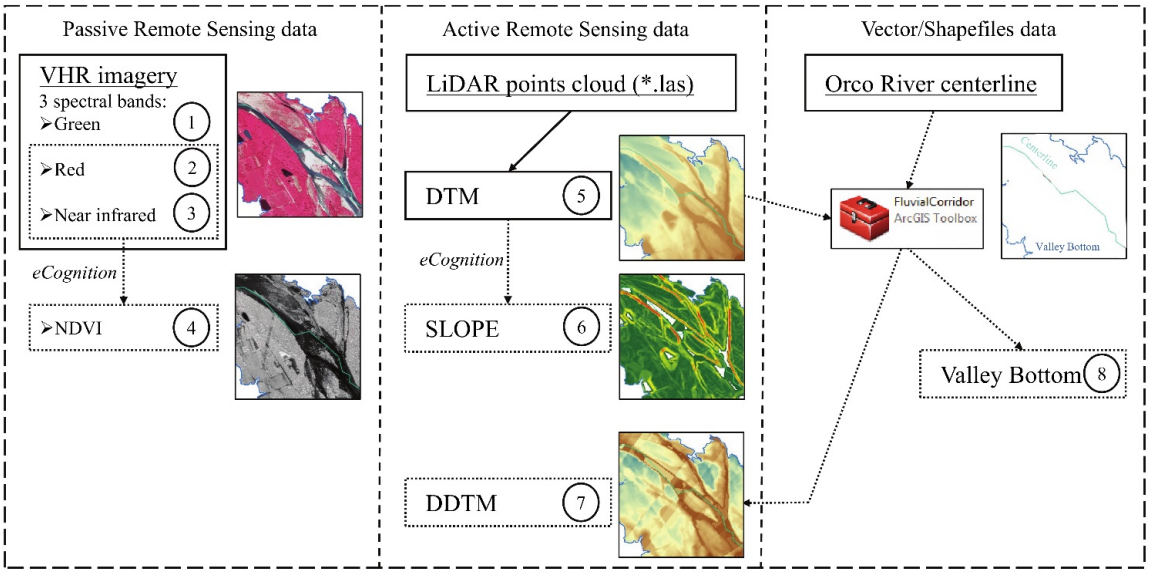

Figure 4. RS and GIS input data used for this study. Dotted lines indicate processes carried out by the authors, while solid lines indicate external processes made available to the authors for the input data preparation.

3. Methodology

3.1. Multilevel GEographical Object-Based Image Analysis (GEOBIA)

The primary aim of GEOBIA is to generate geographic information from RS data that enables users to tackle general environmental issues such as global climate change, natural resource management, landuse/land-cover mapping and others [44]. GEOBIA's ambition as a discipline is to develop theory, methods and tools sufficient to replicate human interpretation of RS imagery in automated/semi-automated ways, allowing for more accurate and repeatable information, less subjectivity, and reduced labor and time costs. GEOBIA relies on RS data and generates GIS outputs, providing a critical bridge between the raster domain of RS and the vector domain of GIS. The "bridge" linking both sides of these domains is the generation of polygons, created by grouping connected pixels with similar characteristics into meaningful image objects, an analysis technique akin to the way humans conceptually organize the landscape to comprehend it [44]. If carefully derived, image objects are closely related to real-world objects [45]. Once objects are derived, topological relationships with other objects, statistical summaries of spectral, textural values, and shape characteristics can all be calculated and employed in the classification procedure. As opposed to pixel-based approaches, the advantage of integrating a broad range of different object features into the analysis process is an improved accuracy for more advanced classification problems [46], such as the ones tackled in this paper.

In this study, we aim to use GEOBIA to enhance the limited spectral resolution of VHR imagery (only Green, Red and Near-infrared bands, see Figure 4) by integrating it with LIDAR-derived topographic information for the multilevel classification of riverscape units and in-stream mesohabitats.

The entire object-based methodology is implemented within eCognition Developer 9® software, from the generation of meaningful objects from the RS data (*i.e.*, image segmentation), to their classification into hydromorphologically meaningful classes.

Because of the strong similarities (both spectrally and topographically) of some of the classes (as explained in Section 2.2), the riverscape units classification problem was tackled in two phases. In the first step (Step 1 of Figure 5), a Machine Learning (ML) object-based classification was developed for mapping the main classes, *i.e.*, Water Channel, Unvegetated Sediment bars, Sparsely-Vegetated units and FloodPlain units (Level 1 of Table 1). Here, the main purpose was to build a supervised classifier able to automatically discern the main land-cover classes found in the active part of the channel (*i.e.*, WC, US and SV from Table 1) from the FloodPlain unit class (FP from Table 1), in order to automatically define the boundaries of the total active channel. For this reason, we propose a multilevel hierarchical segmentation approach based on the two sources of RS data available in order to generate objects that are as closely related to real-world objects. The first level of the hierarchical segmentation (Level 1 of Figure 5) was produced within eCognition using the multi-resolution algorithm [46] with the Slope layer alone (layer 6 of Figure 2). Thereby, different terrain features of similar slope, emerging from ongoing morphological processes of the river, might be distinguishable. A finer sub-level segmentation (Level 2 of Figure 5) was then produced with the multi-resolution algorithm, using the four spectral layers available, equally-weighted: Green, Red and Near infrared spectral bands plus NDVI (respectively layers 1,2,3 and 4 of Figure 2). This step generated image objects of different spectral characteristics within bigger objects that had homogenous slope features. For example, on a sediment bar identified at Level 1 by specific topographic characteristics, sparsely-vegetated patches could possibly be distinguished from bare sediments or from densely-vegetated objects characterized by different spectral values at Level 2. Performing the ML classification on the Level 2 segmentation (Figure 5) might therefore facilitate the challenging task of distinguishing the main land-cover classes found in the active part of the channel (*i.e.*, WC, US and SV from Table 1) from areas of the FP class characterized by very similar spectral characteristics (for instance US in the AC and bare soil crops within the FP). The two-level segmentations were run with the scale parameter set to 40, the shape coefficient at 0.1 and the compactness coefficient set to 0.5. Because of the different spatial resolutions of topographic and spectral data (respectively 5 m and 0.4 m), the same scale parameter used with different input data resulted in smaller objects at the level 2 segmentation, based on spectral differences.

Once the main riverscape units were automatically classified (Level 1 of Table 1) and the active channel boundary was well defined, more detailed vegetation classes (Level 2 of Table 1) were identified. This was done by implementing an expert-based, post-classification phase (Step 2 of Figure 5), built on rule-sets defined by specific object-based criteria and according to the class description of each riverscape unit to be identified (Table 1). Objects classified in Step 1 as SV were re-classified as Riparian Sparsely-Vegetated units (RSV, Table 1) or as Sparsely-Vegetated units of Islands (SVI, Table 1) if their relative border to the FP class was respectively above or below 0.1. From the FP class, objects being surrounded by WC, US or SVI and with a mean NDVI higher than 0.35 were classified as Densely-Vegetated units of Islands (DVI, Table 1). Objects classified as FP with a mean NDVI higher than 0.35 and having a border to WC, US or RSV classes, were classified as Riparian Densely-Vegetated units (RDV, Table 1). Finally, all remaining objects of the FP class were re-labeled as Other Floodplain Units class (OFU, Table 1).

After the riverscape units classification was finalized, a third level object-based segmentation was further realized for all objects classified as Water Channel (Level 3 of Figure 5), again using a multi-resolution segmentation based on the four spectral layers (1–4 of Figure 2). This time the scale parameter was set to 30 in order to obtain smaller objects capable of representing finer spectral differences and to distinguish in-stream mesohabitats typologies that were not visible at larger object scales. A different, ML, object-based classification was performed at Level 3, this time for mapping the in-stream mesohabitats identified at Level 2 of Table 1.

The next section describes the multilevel, ML classification strategies designed to tackle both Step 1 of the riverscape units mapping and the in-stream mesohabitats mapping.

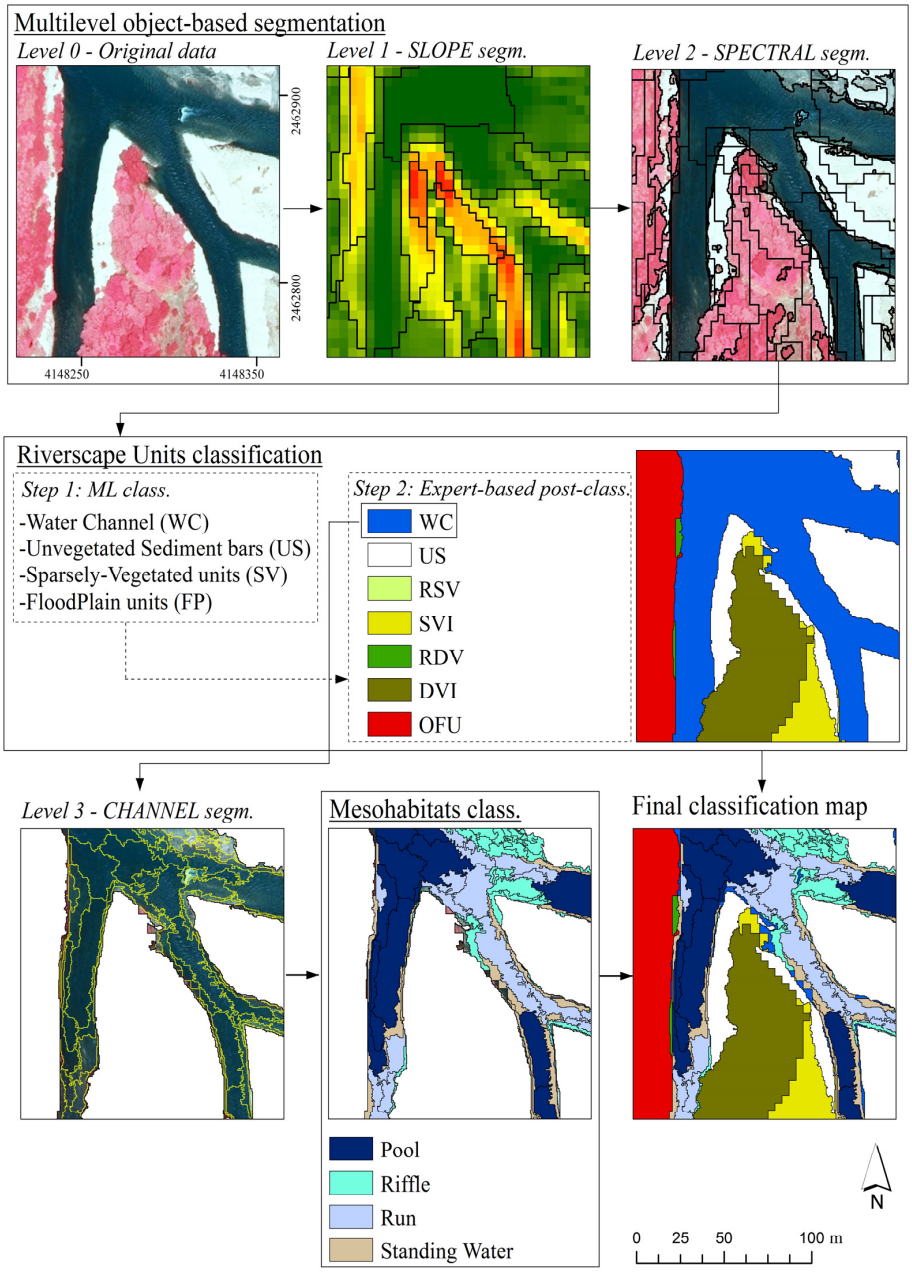

Figure 5. Workflow of the multilevel, object-based methodology developed for the classification of riverscape units and in-stream mesohabitats. Class codes refer to Table 1.

3.2. Multilevel, Machine Learning Classification of Riverscape Units and in-Stream Mesohabitats

A multilevel, supervised classification was performed using Random Forest (RF) [47] and Support Vector Machine (SVM) algorithms. In the field of RS, both classifiers proved to be among the most powerful ML algorithms, especially when classifying high-dimensional pixel-based datasets. In literature, during the recent years they started to be popular also for object-based approaches [48–50]. Moving from pixel-based techniques towards object-based, the feature space data to be classified significantly increases, augmenting the classification complexity and causing problems to standard classifiers traditionally used in object-oriented image analysis, e.g., Nearest Neighbor classifiers.

For this reason, RF and SVM are particularly promising in the context of this study. Object features were calculated for both Levels 2 and 3 segmentations (Figure 5) and grouped in different categories. Different combinations of features were tested with the aim of assessing which produce the highest classification accuracies for either riverscape units or mesohabitat mapping. Table 2 illustrates the different groups of input feature sets calculated. From the VHR imagery, ten "VHR features" (1) were extracted by eCognition software: mean and standard deviation of the four spectral layers (1 to 4 of Figure 2), plus Brightness and Max differences [51]. From the LiDAR-derived products, we grouped the mean and standard deviation of the DTM and Slope (respectively, layers 5 and 6 of Figure 2) as the "LiDAR features" group (2). The mean and standard deviation of the DDTM layer (layer 7 of Figure 2) comprised the "DDTM features" group (3). Fifteen "Geometric features" (4) and twelve "Texture features" (5) were calculated by the eCognition software, the latter based on Haralick [52] and using both GLCM and GLDV approaches on the four spectral layers, among which: homogeneity, contrast, mean, *etc*. For a more detailed explanation of the texture and geometric features calculation, the reader is referred to [51,52].

At the Level 2 segmentation (Figure 5), sample objects were collected based on visual interpretation of VHR imagery, for the Level 1 land-cover classes proposed in Table 1: Water Channel, Unvegetated Sediment bars, Sparsely-Vegetated units and FloodPlain units, resulting in two sets of randomly and spatially-distributed training and validation objects. Table 3 lists the number of samples collected. It is clear that FP class covers most of the analyzed area, and therefore the number of samples collected for this class is much higher than the number of other classes. The training samples collected for the FP class cover 19% of the entire analyzed area, while the validation samples of this class cover 15% of the total area. Considering the whole ground-truthing dataset, the training samples represent about 28% of the whole area and the validation samples about 23% (Table 3). Validation objects were used for the accuracy assessment, based on Kappa values and per-class producer and user accuracy comparisons.

A similar ML approach was also adopted for mapping in-stream mesohabitats, performed at the segmentation Level 3 (see Section 3.1, Figure 5). Training and validation samples were manually collected on VHR imagery, but in this case for the classes: Pools, Riffles, Runs and Standing Waters (Table 1 and Figure 3). A few areas affected by sun glint on water channels surfaces were not included in the training and validation datasets. In this case, several combinations of input features (Table 2) were also tested with the aim of identifying which kinds of features produced the highest classification accuracies for mapping in-stream mesohabitats.

Table 2. Input feature sets used for training different RF and SVM classifiers and for mapping both riverscape units and in-stream mesohabitats.

(1) VHR (10)	(2) LiDAR (4)	(3) DDTM (2)	(4) Geometric (15)	(5) Texture (12)
Mean: -Green -Red -Near infrared -NDVI	**Mean:** -DTM -SLOPE	**Mean:** -DDTM	Area Border length Length Length/Width Width Asymmetry Border index Compactness Density Elliptic fit Radius of largest enclosed ellipse Radius of smallest enclosing ellipse Rectangular fit Roundness Shape index	Homogeneity (GLCM) Contrast (GLCM) Dissimilarity (GLCM) Entropy (GLCM) Angle of 2nd moment (GLCM) Mean (GLCM) Standard deviation (GLCM) Correlation (GLCM) Angle of 2nd moment (GLDV) Entropy (GLDV) Mean (GLDV) Contrast (GLDV)
Standard Deviation: -Brightness -Max difference -Green -Red -Near Infrared -NDVI	**Standard Deviation:** -DTM -SLOPE	**Standard Deviation:** -DDTM		

Table 3. Training and validation samples collected by visual interpretation of VHR imagery and areas covered by each.

	Training			Validation		
	Samples	**Area (km^2)**	**%**	**Samples**	**Area (km^2)**	**%**
WC	2556	1.07	3.6	1504	0.92	3.1
US	2950	0.74	2.5	1990	0.73	2.4
SV	2919	0.74	2.5	1736	0.65	2.2
FP	21761	5.71	19.0	18827	4.56	15.2
			27.5			**22.9**

4. Results and Discussion

4.1. Riverscape Units Classification Results

The results of Step 1 riverscape units classification (Level 1 of Table 1) obtained when testing combinations of different sets of input features (see Table 2) with RF and SVM, are shown in Figure 6. In general, accuracies are very similar for both classifiers, underlying the capability of both ML classifiers to map riverscape units with accuracies in most cases above 0.70. When using the VHR features (group 1 in Table 2), both RF and SVM generate the same Kappa accuracy of 0.79. When the topographic features are utilized alone without any spectral information (LiDAR features and DDTM features, respectively groups 2 and 3 for a total of 6 features), the Kappa accuracy is significantly lower (0.59 for SVM and 0.60 for RF). This is an expected result since spectral information is required for distinguishing Sparsely-Vegetated units from Unvegetated Sediment bars and Water Channel, which could be characterized by similar topographic characteristics but surely different spectral values. Indeed, when combining the spectral features with the topographic ones, Kappa values increase. VHR features together with the LiDAR features (groups 1 and 2 of Table 2, for a total of 14 features) produce a Kappa value of 0.81 for the SVM and 0.78 for the RF. Better performances are generated using DDTM features (group 3, Table 2) with the VHR features (group 1, Table 2), which resulted in a Kappa value of 0.91 for SVM and 0.89 for RF. Using both LiDAR and DDTM features together with the VHR features (groups 1, 2, 3), generates slightly lower accuracies (0.88 for SVM and 0.85 for RF), that might indicate the limits of the algorithms in features selection in the presence of an elevated number of co-varying inputs. When the VHR features are used in combination with the Geometric features (respectively groups 1 and 4, 25 features in total), the accuracy is still relatively high for the RF (0.81), while slightly lower (0.76) for the SVM, showing the limits of SVM in exploiting the Geometric features for this specific classification problem. When VHR features are used with Texture features (respectively groups 1 and 5, 22 features in total) for both classifiers we obtained a Kappa value of 0.84.

These results emphasize the importance of the DDTM layer (layer 7 of Figure 4). Mean and standard deviations of this layer calculated for each object and combined with mean and standard deviations of other spectral layers (layers 1–4 of Figure 4) are sufficient to generate the highest Kappa accuracy when classifying the main riverscape units. The DDTM layer is more important than Geometric features and Texture features (calculated using the four spectral layers). These results underline at the same time the sensibility of the classifiers to the type of features used, rather than the number of features used. In fact, when going from 14 features to 12 (groups 1, 2 to groups 1, 3), the Kappa increases. When going from 12 to 16 features (groups 1, 2, 3) and then to 25 (groups 1, 4), the Kappa gradually decreases.

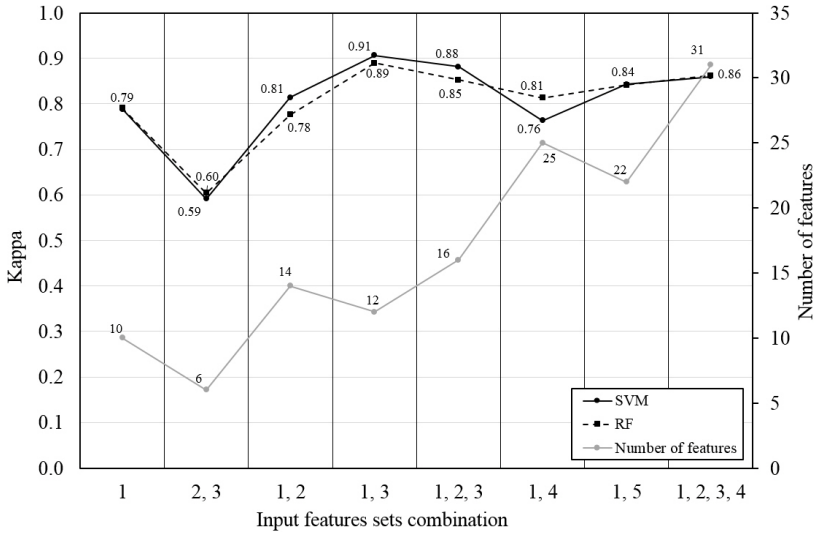

Figure 6. Step 1 riverscape units classification results obtained when testing different combinations of input feature sets (see Table 2) with SVM and RF.

Per-class Producer's (PA) and User's (UA) Accuracies were also analyzed for both classifiers and are plotted in Figure 7. The two classes that produced the highest accuracies were Water Channel and FloodPlain units, which in most cases have PA and UA above 90%. The Sparsely-Vegetated units class is the one with the lowest values of PA and UA among all the experiments. This class presents very similar spectral characteristics to the FP class, due to the presence of vegetation and, at the same time, similar topographic characteristics as the US class. Patches of sparse vegetation are the first stage of the vegetation encroachment, which takes place for some bare sediments (see Section 2.2). When only topographic information are used (groups 2 and 3), the PA and UA reach the lower values, also for the US class. The topographic information supports the delineation of the border between AC classes (WC and US) and the FloodPlain units but cannot distinguish sparse vegetation very well on its own, because this class is characterized by similar topographic features and different spectral features. Only when using the right combination of topographic and spectral input features (in this case spectral and DDTM, groups 1 and 3) is it possible to achieve good accuracy for the SV class.

The most efficient result in terms of Kappa, PA, UA and number of input features was produced by SVM using VHR and DDTM features (groups 1, 3). This result was therefore used in this study for the next steps: step 2 expert-based post-classification and Level 3 segmentation and in-stream mesohabitats classification (see Section 3.1, Figure 5). Commission and Omission Errors were also analyzed for this result (Tables 4 and 5), with the aim of understanding where most of the errors occurred, so they could be removed in the post-processing phase. The Commission Error (CE) of the SV class is 17.25% (see Table 4) meaning that 17.25% of the pixels classified as SV should have been instead classified as other classes, in this case 15.77% of them as the FP class, 1.23% as the WC and 0.25% as the US class. These errors showed that a significant amount of floodplain objects were classified as sparse vegetation. This is most likely due to the similar spectral and topographic values of some vegetation patches occurring in the floodplain, and it indicates that adding the topographic information to the spectral information is not always enough to discern whether an object is located in the floodplain or in the total active channel. This error was significantly reduced by the post-classification step (see Table 4). At the same time, the Omission Error (OE) of the SV class was 21.36% (Table 5), meaning that 21.36% of the SV samples were not classified as SV but labeled as other classes: 19.11% of the pixels as FP, 1.58% as US and 0.67% as WC (Table 5). This misclassification occurs predominantly for the vegetation patches located within the TAC boundaries, underlying some of the limits of the classifier in discerning between sparse and dense vegetation that can be found in the FP class. This type of error, however, would have little effect on hydromorphological characterization.

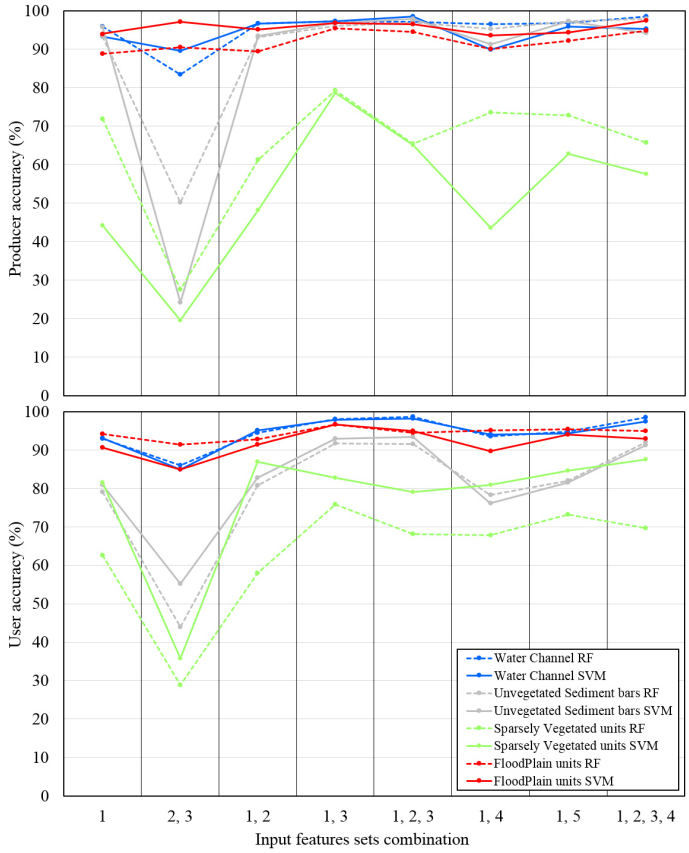

Figure 7. Per-class Producer's and User's Accuracies of riverscape units classes, obtained when testing different combinations of input features sets (see Table 2) with SVM and RF.

The step 2 post-classification phase (Step 2 of Figure 5) developed to classify the Level 2 riverscape units described in Table 1, was also meant to remove the main CE and OE and to reduce the typical "salt and pepper" effect of small objects. In order to reduce the CE and OE errors, several rule-sets were developed following an expert-based approach, under eCognition software. Several attempts were tested in order to obtain the optimal expert-based solution. For example, the CE of the US class was improved by imposing two threshold conditions: distance to WC $\geqslant$ 200 pxl and Mean DDTM value $\geqslant$ 250. US objects satisfying these conditions where labeled as FP class. Thanks to the post-classification phase, the Kappa accuracy was increased from 0.91 to 0.95, the total CE of the SV class reduced from 17.25% to 4.98% (Table 4), and at the same time the OE from 21.36% to 15.39% (Table 5). For the US class the total CE decreased from 7.15% to 3.87%, (Table 4) and the OE decreased from 3.19% to 1.85% (Table 5).

Table 4. Commission Errors (CE) produced by SVM when classifying riverscape units using "VHR and DDTM features" before (above) and after (below) the Step 2 expert-based post-classification.

		Total	FP	US	WC	SV
CE before post-classification	**FP**	3.38	-	0.45	0.19	2.74
	US	7.15	4.65	-	1.15	1.35
	WC	2.14	1.51	0.15	-	0.48
	SV	17.25	15.77	0.25	1.23	-
CE after post-classification	**FP**	2.13	-	0.23	0.17	1.73
	US	3.87	1.07	-	1.29	1.51
	WC	1.41	0.78	0.15	-	0.48
	SV	4.98	3.31	0.30	1.37	-

Table 5. Omission Errors (OE) produced by SVM when classifying riverscape units using "VHR and DDTM features" before (above) and after (below) the Step 2 expert-based post-classification.

		Total	FP	US	WC	SV
OE before post-classification	**FP**	3.23	-	0.78	0.30	2.15
	US	3.19	2.80	-	0.18	0.21
	WC	2.70	0.92	0.95	-	0.83
	SV	21.36	19.11	1.58	0.67	-
OE after post-classification	**FP**	0.74	-	0.18	0.16	0.40
	US	1.85	1.43	-	0.19	0.23
	WC	2.66	0.83	1.03	-	0.80
	SV	15.39	12.84	1.82	0.73	-

The step 2 post-classification phase also visually enhanced the spatial patterns of the final riverscape units map in some locations. Figure 8 shows an example of CE for the US and WC classes, after the Step 1 ML classification with SVM. The mining activities localized in the floodplain were not classified as FP but as US (white color), probably due to the high spectral and topographic similarities, since the mining site is located close to the active channel area and therefore at a similar elevation. Similarly, the water pond found in the floodplain was classified as WC instead of FP (blue color). These errors were not abundant and only occasional: in this case, 4.65% CE for US class in the FP class, and 1.51% CE for WC class in the FP class. Therefore, the post-classification phase is an important resource for deleting this type of bias, which at some locations cannot be eliminated by exploiting the spectral and topographic information alone. At the same time, the expert-based rule-sets developed based on object-neighboring and spectral characteristics allowed us to map riverscape units at a higher level, by distinguishing all the vegetation classes composing the natural fluvial corridor (Level 2, Table 1). Although this object-based, rule-set architecture developed was case-specific and could have been influenced by operators' subjectivity, it proved to be very efficient and flexible. Designing *ad-hoc* solutions, suitable to solve specific classification problems, is relatively simple within GEOBIA, as it is demonstrated by these results.

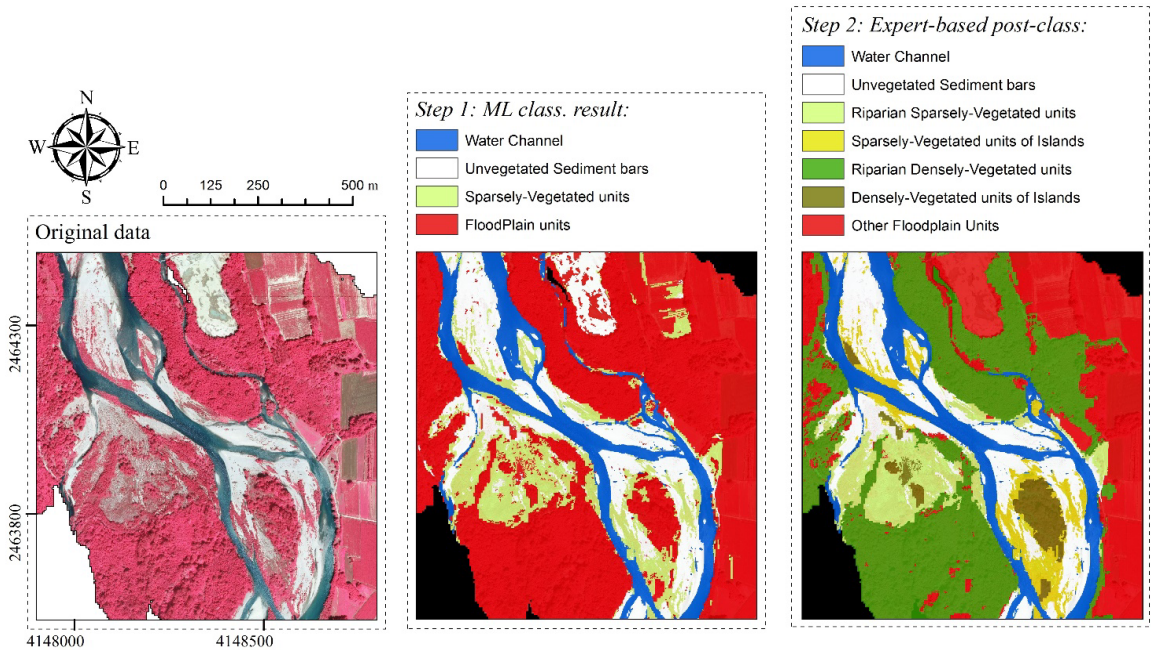

Figure 8. Example of riverscape units classification results: Step 1 obtained with SVM and Step 2 improvements after post-processing.

4.2. In-Stream Mesohabitat Classification Results

From the WC class obtained at the segmentation Level 2, a finer Level 3 segmentation was produced for the classification of in-stream mesohabitats (see Section 3.1, Figure 5). Several combinations of input feature sets (Table 2) calculated for the Level 3 objects were combined and assessed in terms of Kappa accuracy for both RF and SVM classifiers (as already explained in Section 3.1). DDTM features do not exist for the channel class, since relative altitude differences are calculated with respect to the main river channel. Results are plotted in Figure 9. In general, SVM slightly out-performs RF. For both classifiers, the lowest accuracies were obtained using VHR features alone (group 1). When VHR features were combined with one of the other input features group, the classification performances likewise improved. The best accuracy when using two groups of input features achieved a Kappa value of 0.77 by combining Texture and VHR features (groups 1 and 5) for both RF and SVM, while the lowest accuracy was obtained using VHR and LiDAR features (0.70 for RF and 0.71 for SVM). When spectral features were combined with two other groups of features at the same time, the accuracy was always around 0.80 for SVM. RF results were slightly more sensitive to the input feature group used.

Looking at the PA and UA of the mesohabitat classes (Figure 10), one notes that Riffles are better identified. This is most likely due to the turbulence of the water that creates a very distinct spectral signal. Pools and Standing Waters have the highest rate of misclassification, since both are characterized by still or slow flowing water. Some misclassifications of the class Runs are also expected being a transitional class between riffles and pools. Using the SVM classifier with Geometric and Texture features (groups 1, 4 and 5) seems to be the best combination since in this case all mesohabitats classes have PA and UA values higher than 75%. In other words, for mesohabitats classification, spectral texture and geometric features significantly enhance the classifier performances. These results demonstrate the strength of the GEOBIA approach, which enables the enrichment of the limited spectral information with object-related features specific to a particular classification problem.

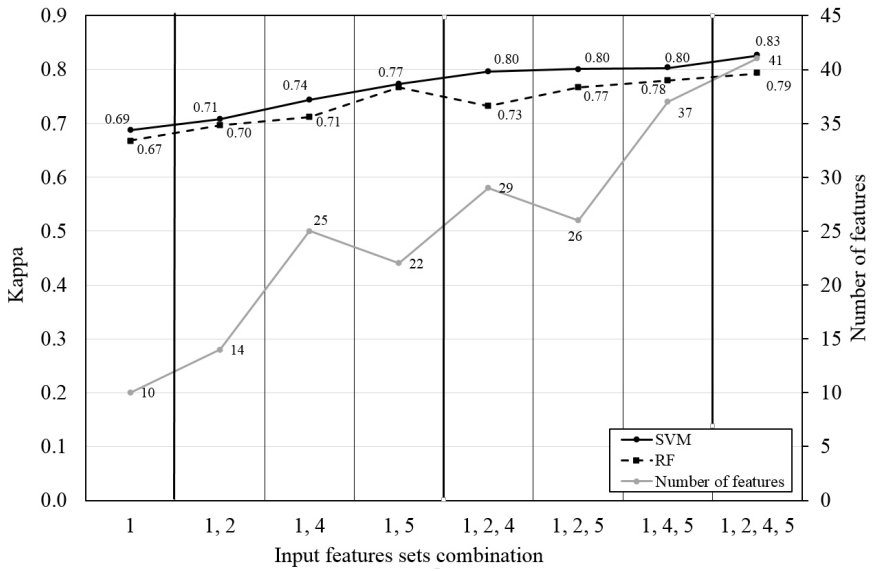

Figure 9. In-stream mesohabitats classification results obtained when testing combinations of different input feature sets (see Table 2) with SVM and RF.

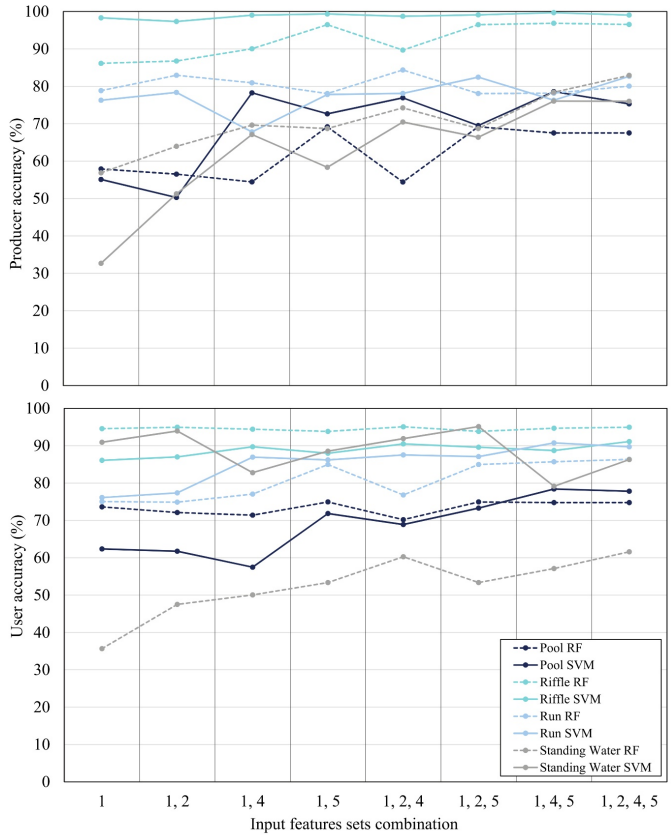

Figure 10. Per-class Producer's and User's Accuracies of mesohabitats classes, obtained when testing combinations of different input feature sets (see Section 3.2) with SVM and RF.

4.3. New Perspectives in Hydromorphological Characterization of Rivers

Traditionally, riverine hydromrophological characterization relied on data collected via field surveys. Although very informative, these data are often discontinuously scattered along the river network and are dependent on operator expertise and subjectivity. In this context, RS information, in particular orthophotos, have notably enriched the ability to analyze fluvial processes and channel adjustment trajectories over the past several decades, especially with regard to exploiting historical archives of aerial imageries [20,53]. These approaches visually and manually classify visible river features from orthophotos. This is time and resource consuming and for this reason has been mostly applied on selected river courses. Moreover, advances in remote sensing technology nowadays provide multiple layers of information ranging from multiple spectral bands to topography, which cannot be properly investigated simply by visual interpretation.

Figure 11 shows an example of an analysis that can be conducted using the produced RS classification of riverscape units with the methodology proposed in this paper. In the top of the figure, two classification maps show reaches representative of the two river types occurring along the analyzed stretch. Along the first 20 km, the river presents a sinuous, single-thread channel, which afterwards turns into wandering channels (multiple channels separated by unvegetated and vegetated bars). Each point in the scatter plots represents a segmented object. In terms of areal features, the scatter plots provide information on length–width ratio and rectangular index. Based on Unvegetated Sediment bars, the changes in channel features between the two river types are clearly visible, around the 20th km. For the wandering river type, the distribution of sediment bars significantly widens, with longer bars with higher length–width ratios. The rectangular index also decreases for longer forms, indicating that enlarged Unvegetated Sediment bars are wider in the center and narrower toward their extremities (see classification maps on the top of the Figure 11). On the other hand,

Densely-Vegetated units of Islands regularly occur only in the wandering river type. Bigger islands, with higher length–width ratios, seems to have a kind of periodicity, although a proper assessment of periodicity is out of the scope of this analysis. Note that the rectangular index here is homogenous, indicating that the object shape is mostly rectangular for DVI objects. The bottom scatter plot provides information on topography. It reports the longitudinal patterns of mean DDTM for the US class, in other words the average bar elevations. Two significantly different morphological signatures describe the two river types: average bar elevations from the Water Channel and mean slope of the US objects are systematically higher for sinuous single-channel type compared to wandering. It is also possible to spot a systematic tendency to decrease the value of mean DDTM going downstream.

This type of analysis provides a continuous, objective and repeatable mapping of hydromorphological indicators in terms of areal geometry and topography. If sequential acquisitions of the same kind become more common and available in the future, this approach will open novel possibilities for monitoring fluvial processes in an unprecedented way.

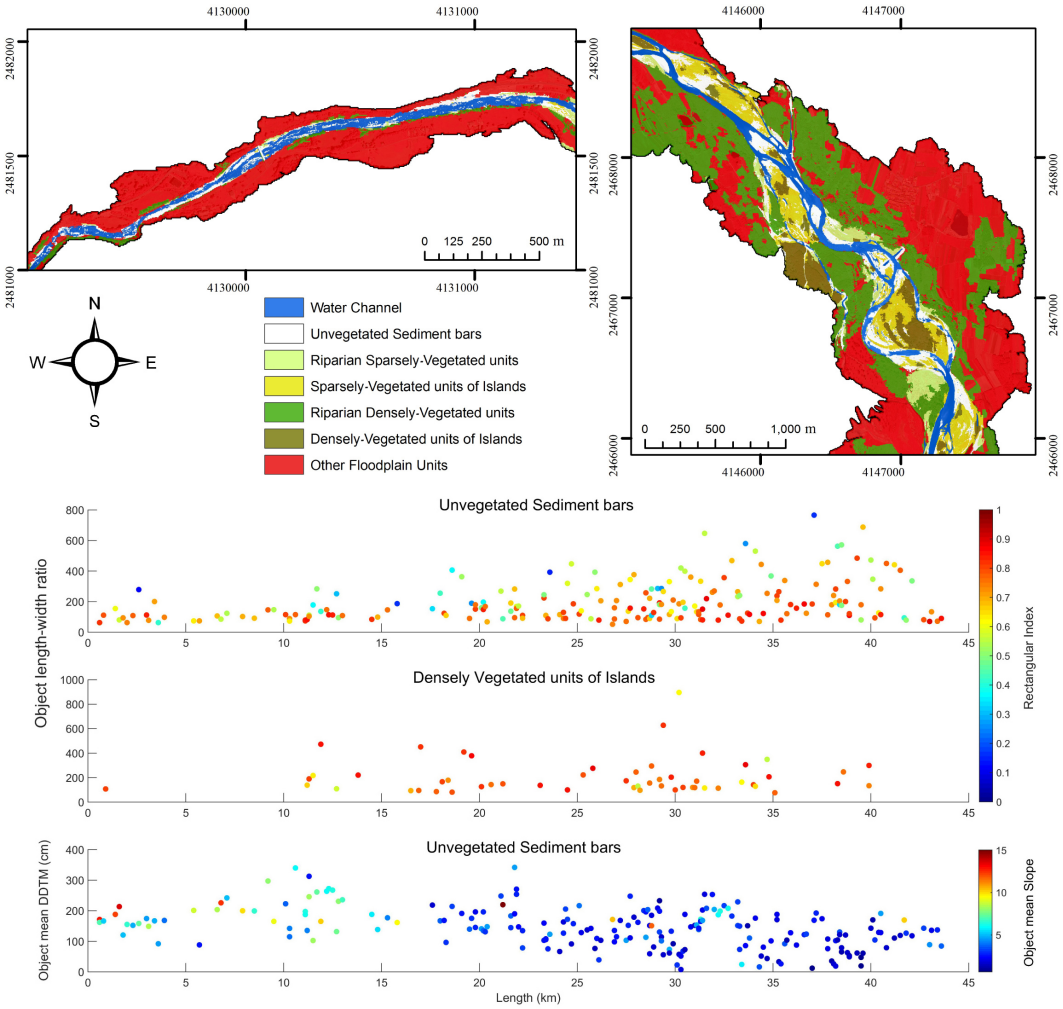

Figure 11. Longitudinal patterns of object features distinguished for different riverscape units. The first (from the **top**) two scatter plots show length–width ratios for the Unvegetated Sediment bars and Densely-Vegetated units of Islands classes. Dot colors are proportional to the rectangular index. The third scatter plot shows the pattern of mean DDTM for US class, dot colors are proportional to the object mean slope. The top pictures show examples of riverscape unit classification for the two river types present: sinuous, single-thread channel (picture on the **left**) which turns into wandering channel (picture on the **right**) near the 20th km analyzed.

5. Conclusions

The multilevel GEOBIA framework presented in this paper proves to be a new powerful tool for semi-automated classification of essential geomorphic features, in particular for the characterization of the natural fluvial corridor, the delineation of the active river channel, and for in-stream mesohabitat mapping. GEOBIA allows for the integration of different sources of RS data, such as VHR imagery and LiDAR data, in a flexible but robust environment. Thanks to its hierarchical, multilevel capability, the potentials of VHR imagery and LiDAR data are exploited at each level in different ways by combining different object features. Compared to previous studies that solely applied spectral information for a similar classification target [8,22,54], here for the first time spectral and topographic information have been hierarchically integrated for the characterization of the riverscape units providing a number of benefits. First, the method performances are higher than all previous attempts reported in literature (best performances result in K values of 0.91 for riverscape units and 0.83 for in-stream mesohabitats), although validation datasets are subject to the operator subjectivity and therefore present difficult comparisons. Second, the method proposed allows to automatically delineate the active river channel boundary from other floodplain units, at the same time mapping all the vegetation units within the riverscape environment, such as Riparian Densely-Vegetated units or Sparsely-Vegetated units of Islands. These classes have a hydromorphological meaning of key importance, and, in cases where sequential acquisitions of the same kind might be available, the proposed methodology would be a more objective monitoring tool for tracking changes in fluvial processes.

The Machine Learning classification results show that topographical information is a relevant data source that enhances the identification accuracy of the main riverscape units (Water Channel, Unvegetated Sediment bars, Sparsely-Vegetated units, FloodPlain units). In particular, the Detrended Digital Terrain Model (DDTM), which reports the elevation of the objects with respect to the river network. The best performance of mapping riverscape units was produced when VHR and DDTM features were combined, for both SVM and RF. The DDTM is a powerful descriptor of AC-Floodplain connectivity and enables the classifiers to discern between different riverscape elements with similar spectral signatures: for example a bar of bare sediments within the AC and a bare arable crop field in the floodplain, or a patch of sparse vegetation in the AC and a sparsely-vegetated area in the floodplain. The per-class Producer's and User's Accuracies demonstrate that the AC boundary might be successfully delineated from topographic information alone, but only when using the right combination of input features (in this case VHR and DDTM), it is also possible to gather high accuracies in a similar fashion for the Sparsely-Vegetated units. Most confusion occurs, in fact, between floodplain and sparse vegetation classes, both within and outside the active channel boundaries, probably due to the difficulty in distinguishing between vegetation patches that might appear in both cases. However, the use of spectral information enriched by geometric or texture features obtained by the object-oriented approach achieves satisfactory classification results as well; see, for instance, the Kappa value of 0.84 for both SVM and RF, obtained using VHR and Texture features (Figure 6). This result might be explained by the fact that the first level segmentation (see Figure 5) was based on the slope layer alone, allowing us to create meaningful topographic objects to be classified. This first-level segmentation provided meaningful morphological patterns of river forms, such as the longitudinal developments of DDTM for the unvegetated sediment bars discussed in Figure 11. These kinds of assessments, which hold notable potentials for monitoring fluvial geomorphological processes in the near future, can be obtained only by integrating topography with spectral information. Indeed, the border of an object derived by segmentation based purely on spectral information might not take into account the topographic variability, important information that would otherwise be lost. For example, a uniformly vegetated area adjacent to the river characterized by an increasing slope would generate a uniform object if segmentation was based solely on spectral features. Adding the topographic segmentation allows generating various objects with different topographic characteristics, which is of key importance in hydromorphological terms.

The GEOBIA architecture also allows for the design of *ad-hoc*, object-based rule-sets, which are able to increase the level of details of some vegetation classes in the riverscape environment and to solve specific classification problems, such as the ones mentioned above, in a relatively simple way.

The classification of in-stream mesohabitats also achieved promising results producing the best Kappa value of 0.83 when classifying spectral, topographic, geometric and texture features with SVM. Here, the spectral texture and geometric features produce similar performances compared to previous attempts in literature that used a similar GEOBIA approach [22]. Thanks to the very high spatial resolution of the near-infrared imagery as well as the object-based approach, which allows to enhance the limited spectral resolution by adding texture and geometric features, mapping of the main in-stream mesohabitats can now be done with a high level of accuracy, without the need for hyperspectral data, a major enhancement compared to previous results in literature that used this type of data [28]. In addition, in this case, it is reasonable to suppose that the first level of segmentation based on slope facilitated the classification exercise by building precise objects already belonging to specific mesohabitats to be classified: riffle and pools correspond respectively to areas of higher and respectively lower slopes in the riverbed profile. However, an important limitation when classifying in-stream mesohabitats is the effect of sun glint. Some areas affected by this phenomenon were neglected in this study. However, for future large-scale applications, this aspect needs to be addressed more systematically.

We believe that the semi-automated GEOBIA framework proposed in this paper provides notable potential to enrich the availability of hydromorphological data, opening novel perspectives in the river science, which has been characterized so far by a chronic lack of suitable river geomorphological data over large scales and through time [55]. The application of the proposed method to the entire Piedmont Region, where the same dataset is already available, is now a logical and feasible possibility. Similar datasets are nowadays starting to be available for most European Member States [33] and most Member States have already planned similar RS acquisition campaigns in the future. In this context, and considering the remarkable method's flexibility to the use of different RS input features, there will be ample opportunities to broadly apply the proposed technique. If classification of riverscape units and in-stream mesohabitats will be applied in the future at regional scales around Europe and repeated through time, it will yield an unprecedented dataset of continuous riverscape features that would allow monitoring and characterizing the hydromorphological status of river systems coherently through time in a semi-automated way. This would become a valuable source of data for fluvial geomorphologists: it would allow, for instance, for the design of survey campaigns and restoration targets based on quantitative, objective and repeatable indicators, an urgent and challenging requirement of the WFD, which has not yet been addressed by European Member States.

Acknowledgments: We thank Robin Jenkinson (CNRS) for reviewing the manuscript and our colleague Christof Weissteiner for helping in the initial phase of the manuscript conception. This work would not have been possible without the courtesy of Regione Piemonte, which provided the free accessibility to this dataset, in particular Silvestro, Siletto and Campus.

Author Contributions: Luca Demarchi conceived and designed the methodology and analyzed the remote sensing database, producing and assessing the final riverscape units and in-stream mesohabitats mapping. Simone Bizzi contributed to the supervision of the whole methodology from the hydromorphological perspective. Hervé Piégay supervised the study and reviewed the manuscript. All authors read and approved the manuscript.

Conflicts of Interest: The authors declare no conflict of interest.

References

1. Brierley, G.J.; Fryirs, K.A. *Geomorphology and River Management: Applications of the River Styles Framework*; Blackwell: Oxford, UK, 2005.
2. Rinaldi, M.; Surian, N.; Comiti, F.; Bussettini, M. A method for the assessment and analysis of the hydromorphological condition of Italian streams: The Morphological Quality Index (MQI). *Geomorphology* **2013**, *180*, 96–108. [CrossRef]

3. Gurnell, A.M.; Rinaldi, M.; Belletti, B.; Bizzi, S.; Blamauer, B.; Braca, G.; Buijse, T.; Bussettini, M.; Camenen, B.; Comiti, F.; *et al*. A multi-scale hierarchical framework for developing understanding of river behaviour to support river management. *Acquat. Sci.* **2016**, *78*, 1–16.
4. European Commission. Directive 2000/60/EC of the European Parliament and of the Council establishing a framework for Community action in the field of water policy. *Off. J. Eur. Union* **2000**, *327*, 1–73.
5. Carbonneau, P.E.; Piégay, H. *Fluvial Remote Sensing for Science and Management*; Carbonneau, P.E., Piégay, H., Eds.; John Wiley & Sons, Ltd: Chichester, UK, 2012.
6. Marcus, W.A.; Fonstad, M.A. Remote sensing of rivers: The emergence of a subdiscipline in the river sciences. *Earth Surf. Process. Landf.* **2010**, *35*, 1867–1872. [CrossRef]
7. Buffington, J.M.; Montgomery, D.R. Geomorphic classification of river. In *Treatise on Geomorphology*; Shroder, J., Wohl, E., Eds.; Elsevier: San Diego, CA, USA, 2013; pp. 730–767.
8. Bertrand, M.; Piégay, H.; Pont, D.; Liébault, F.; Sauquet, E. Sensitivity analysis of environmental changes associated with riverscape evolutions following sediment reintroduction: Geomatic approach on the Drôme River network, France. *Int. J. River Basin Manag.* **2013**, *11*, 19–32. [CrossRef]
9. Alber, A.; Piégay, H. Spatial disaggregation and aggregation procedures for characterizing fluvial features at the network-scale: Application to the Rhône basin (France). *Geomorphology* **2011**, *125*, 343–360. [CrossRef]
10. Belletti, B.; Dufour, S.; Piégay, H. What is the relative effect of space and time to explain the braided river width and island patterns at a regional scale? *River Res. Appl.* **2013**. [CrossRef]
11. Marcus, W.A.; Fonstad, M.A.; Legleiter, C.J. management applications of optical remote sensing in the active river channel. In *Fluvial Remote Sensing for Science and Management*; Carbonneau, P., Piegay, H., Eds.; John Wiley & Sons, Ltd.: Chichester, UK, 2012; pp. 19–42.
12. Ham, D.; Church, M. *Channel Island and Active Channel Stability in the Lower Fraser River Gravel Reach*; University of British Columbia: Vancouver, BC, Canada, 2002.
13. Toone, J.; Rice, S.P.; Piégay, H. Spatial discontinuity and temporal evolution of channel morphology along a mixed bedrock-alluvial river, upper Drôme River, southeast France: Contingent responses to external and internal controls. *Geomorphology* **2014**, *205*, 5–16. [CrossRef]
14. Gurnell, A.M.; Petts, G.E.; Hannah, D.M.; Smith, B.P.G.; Edwards, P.J.; Kollmann, J.; Ward, J.V.; Tockner, K. Riparian vegetation and island formation along the gravel-bed Fiume Tagliamento, Italy. *Earth Surf. Process. Landf.* **2001**, *26*, 31–62. [CrossRef]
15. Wintenberger, C.; Rodrigues, S.; Villar, M.; Bréhéret, J.G. The key role of pioneer woody vegetation in mid-channel bar metamorphosis to island: Case study from the River Loire (France). In Proceedings of the 10th International Conference on Fluvial Sedimentology, Leeds, UK, 14–19 July 2013; pp. 2–3.
16. Osterkamp, W.R. Processes of fluvial island formation, with examples from Plum Creek, Colorado and Snake River, Idaho. *Wetlands* **1998**, *18*, 530–545. [CrossRef]
17. Arnaud, F.; Piégay, H.; Schmitt, L.; Rollet, A.J.; Ferrier, V.; Béal, D. Historical geomorphic analysis (1932–2011) of a by-passed river reach in process-based restoration perspectives: The Old Rhine downstream of the Kembs diversion dam (France, Germany). *Geomorphology* **2015**, *236*, 163–177. [CrossRef]
18. Piégay, H.; Darby, S.A.; Mosselmann, E.; Surian, N. The erodible corridor concept: Applicability and limitations for river management. *River Res. Appl.* **2005**, *21*, 773–789. [CrossRef]
19. Bollati, I.M.; Pellegrini, L.; Rinaldi, M.; Duci, G.; Pelfini, M. Reach-scale morphological adjustments and stages of channel evolution: The case of the Trebbia River (northern Italy). *Geomorphology* **2014**, *221*, 176–186. [CrossRef]
20. Liébault, F.; Piegay, H. Assessment of channel changes due to long term bedload supply decrease, Roubion River, France. *Geomorphology* **2001**, *36*, 167–186. [CrossRef]
21. Legleiter, C.J. Remote measurement of river morphology via fusion of LiDAR topography and spectrally based bathymetry. *Earth Surf. Process. Landf.* **2012**, *37*, 499–518. [CrossRef]
22. Wiederkehr, E.; Belletti, B.; Dufour, S.; Piégay, H. Physical characterisation of river corridors from orthophotos: Challenging issues and first application to the Rhône hydrographical network. In Proceedings of the GEOBIA 2010-Geographic Object-Based Image Analysis Conference, Ghent, Belgium, 29 June–2 July 2010; pp. 1682–1777.
23. Vezza, P.; Parasiewicz, P.; Spairani, M.; Comoglio, C. Habitat modeling in high-gradient streams: The mesoscale approach and application. *Ecol. Appl.* **2014**, *24*, 844–861. [CrossRef] [PubMed]

24. Frissell, C.; Liss, W.J.; Warren, C.E.; Hurley, M.D. A hierarchical framework for stream habitat classification: Viewing streams in a watershed context. *Environ. Manag.* **1986**, *10*, 199–214. [CrossRef]
25. European Commission. Directive 1992/43/EEC on the conservation of natural habitats and of wild fauna and flora. *Off. J. Eur. Union* **1992**, *389*, 7–50.
26. Acreman, M.C.; Ferguson, A.J.D. Environmental flows and the European Water Framework Directive. *Freshw. Biol.* **2010**, *55*, 32–48. [CrossRef]
27. Vezza, P.; Goltara, A.; Spairani, M.; Zolezzi, G.; Siviglia, A.; Carolli, M.; Cristina Bruno, M.; Boz, B.; Stellin, D.; Comoglio, C.; *et al*. Habitat indices for rivers: Quantifying the impact of hydro-morphological alterations on the fish community. In *Engineering Geology for Society and Territory—Volume 3 SE—75*; Lollino, G., Arattano, M., Rinaldi, M., Giustolisi, O., Marechal, J.-C., Grant, G.E., Eds.; Springer International Publishing: Basel, Switzerland, 2015; pp. 357–360.
28. Wright, A.; Marcus, W.A.; Aspinall, R. Evaluation of multispectral, fine scale digital imagery as a tool for mapping stream morphology. *Geomorphology* **2000**, *33*, 107–120. [CrossRef]
29. Legleiter, C.J.; Marcus, W.A.; Rick, L. Effects of sensor resolution on mapping instream habitats. *Photogramm. Eng. Remote Sens.* **2002**, *68*, 801–807.
30. Marcus, W.A.; Legleiter, C.J.; Aspinall, R.J.; Boardman, J.W.; Crabtree, R.L. High spatial resolution hyperspectral mapping of in-stream habitats, depths, and woody debris in mountain streams. *Geomorphology* **2003**, *55*, 363–380. [CrossRef]
31. Weng, Q.; Hu, X.; Lu, D. Extracting impervious surfaces from medium spatial resolution multispectral and hyperspectral imagery: A comparison. *Int. J. Remote Sens.* **2008**, *29*, 3209–3232. [CrossRef]
32. Demarchi, L.; Canters, F.; Chan, J.C.-W.; van de Voorde, T. Multiple endmember unmixing of CHRIS/Proba imagery for mapping impervious surfaces in urban and suburban environments. *IEEE Trans. Geosci. Remote Sens.* **2012**, *50*, 3409–3424. [CrossRef]
33. Bizzi, S.; Demarchi, L.; Grabowski, R.; Weissteiner, C.; van de Bund, W. The use of remote sensing to characterise hydromorphological properties of European rivers. *Aquat. Sci.* **2016**, *78*, 57–70. [CrossRef]
34. Regione Piemonte. *Piano di Tutela Della Acque-Allegato Tecnico II.h/1-Bilancio Delle Disponibilità Idriche Naturali e Valutazione Dell'incidenza dei Prelievi*; Regione Piemonte: Turin, Italy, 2004.
35. Turitto, O.; Audisio, C.; Agangi, A. Il ruolo svolto da piene straordinarie nel rimodellare la geometria di un alveo fluviale. *Ital. J. Quat. Sci.* **2008**, *21*, 303–316.
36. Pellegrini, L.; Maraga, F.; Turitto, O.; Audisio, C.; Duci, G.; Pavia, U.; Ferrata, V. Evoluzione morfologica di alvei fluviali mobili nel settore occidentale del bacino padano. *Ital. J. Quat. Sci.* **2008**, *21*, 251–266.
37. Weng, Q. Remote sensing of impervious surfaces in the urban areas: Requirements, methods, and trends. *Remote Sens. Environ.* **2012**, *117*, 34–49. [CrossRef]
38. Herold, M.; Roberts, D.A.; Gardner, M.E.; Dennison, P.E. Spectrometry for urban area remote sensing—Development and analysis of a spectral library from 350 to 2400 nm. *Remote Sens. Environ.* **2004**, *91*, 304–319. [CrossRef]
39. Dennison, P.E.; Roberts, D.A.; Regelbrugge, J. Characterizing chaparral fuels using combined hyperspectral and synthetic aperture radar. In Proceedings of the 9th JPL Airborne Earth Science Workshop, Pasadena, CA, USA, 23–25 February 2000; pp. 119–124.
40. European Commission. Directive 2007/2/EC of the European Parliament and of the Council of 14 March 2007 establishing an Infrastructure for Spatial Information in the European Community (INSPIRE). *Off. J. Eur. Union* **2007**, *108*, 1–14.
41. Zevenbergen, L.W.; Thorne, C.R. Quantitative analysis of land surface topography. *Earth Surf. Process. Landf.* **1987**, *12*, 47–56. [CrossRef]
42. Roux, C.; Alber, A.; Bertrand, M.; Vaudor, L.; Piégay, H. "FluvialCorridor": A new ArcGIS toolbox package for multiscale riverscape exploration. *Geomorphology* **2015**, *242*, 29–37. [CrossRef]
43. Notebaert, B.; Piégay, H. Multi-scale factors controlling the pattern of floodplain width at a network scale: The case of the Rhône basin, France. *Geomorphology* **2013**, *200*, 155–171. [CrossRef]
44. Hay, G.J.; Castilla, G. Geographic object-based image analysis (GEOBIA): A new name for a new discipline. In *Lecture Notes in Geoinformation and Cartography*; Springer Berling Heidelberg: Heidelberg, Germany, 2008; pp. 75–89.
45. Platt, R.V.; Rapoza, L. An evaluation of an object-oriented paradigm for land use/land cover classification. *Prof. Geogr.* **2008**, *60*, 87–100.

46. Benz, U.C.; Hofmann, P.; Willhauck, G.; Lingenfelder, I.; Heynen, M. Multi-resolution, object-oriented fuzzy analysis of remote sensing data for GIS-ready information. *ISPRS J. Photogramm. Remote Sens.* **2004**, *58*, 239–258. [CrossRef]
47. Breiman, L. Random forests. *Mach. Learn.* **2001**, *45*, 5–32. [CrossRef]
48. Tzotsos, A.; Argialas, D. Support vector machine classification for object-based image analysis. In *Object Based Image Analysis*; Springer Berlin Heidelberg: Heidelberg, Germany, 2008; pp. 663–677.
49. Xun, L.; Wang, L. An object-based SVM method incorporating optimal segmentation scale estimation using Bhattacharyya Distance for mapping salt cedar (Tamarisk spp.) with QuickBird imagery. *GISci. Remote Sens.* **2015**, *52*, 257–273. [CrossRef]
50. Heumann, B.W. An object-based classification of mangroves using a hybrid decision tree—Support vector machine approach. *Remote Sens.* **2011**, *3*, 2440–2460. [CrossRef]
51. eCognition Developer, Trimble. *9.0 User Guide*; Trimble Germany GmbH: Munich, Germany, 2014.
52. Haralick, R.M. Statistical and structural approach to texture. *Proc. IEEE* **1979**, *67*, 786–804. [CrossRef]
53. Surian, N.; Rinaldi, M. Morphological response to river engineering and management in alluvial channels in Italy. *Geomorphology* **2003**, *50*, 307–326. [CrossRef]
54. Belletti, B.; Dufour, S.; Piégay, H. Regional variability of aquatic pattern in braided reaches (example of the French Rhône basin). *Hydrobiologia* **2012**, *712*, 25–41. [CrossRef]
55. Schmitt, R.; Bizzi, S.; Castelletti, A. Characterizing fluvial systems at basin scale by fuzzy signatures of hydromorphological drivers in data scarce environments. *Geomorphology* **2014**, *214*, 69–83. [CrossRef]